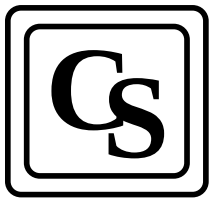

COMPUTER SCIENCE TECHNICAL REPORT

Discretizing Aerosol Dynamics with B-Splines

Adrian Sandu and Christian Borden

CSTR-01-09
December 2001

Michigan Technological University, Houghton, MI 49931

Discretizing Aerosol Dynamics with B-Splines

Adrian Sandu* and Christian T. Borden

Department of Computer Science, Michigan Technological University,
Houghton, MI 49931. E-mail {asandu,ctborden}@mtu.edu.

*Corresponding author.

Abstract

This paper presents a discretization technique for particle dynamics equation based on the B-spline interpolation of the solution. The method is developed in the general framework recently proposed by the authors, and extends the previous work of Pilinis and Seinfeld to arbitrary order splines and arbitrary knot sequences. Numerical tests include the coagulation-growth of the exponential distribution and of a cosine hill in logarithmic coordinates.
Keywords: Aerosol dynamics, B-spline interpolation.

1 Introduction

As our understanding expands, new processes are incorporated into air quality computer models. One example is the particulate matter (aerosol) processes, the importance of which is now widely recognized. Aerosols are now a priority focus area in environmental science due to the leading role they play as a cause of adverse human health, and their ability to scatter and absorb incoming solar radiation and thus modify warming due to greenhouse gases and reduce visibility. Particulate matter (aerosol) processes are "emerging as a new frontier" in environmental studies (Nobel laureate P. Crutzen et. al. [6]).

To accurately study the effects of aerosols it is necessary to resolve aerosol number and mass distributions as a function of chemical composition and size. Treatment of aerosol processes leads to (at least) an order of magnitude increase in the overall computational time of an air quality model; this is mainly due to repeatedly solving the aerosol chemistry (or chemical equilibria) for different particle sizes. Therefore there is a clear need for rigorous, reliable and efficient computational techniques for aerosol simulations. In particular, there is a need for methods that accurately solve aerosol dynamics using a small number of size bins (discretization points), such that the time for aerosol chemistry calculations (which is proportional to the number of bins) is manageable.

In this paper we develop a family of methods for solving the aerosol dynamics equations based on a semi-discretization in particle size followed by the time-stepping method of choice. The semi-discretization in size follows the general framework we proposed earlier [25]; the particular class of methods developed here approximate the solution by a B-spline polynomial interpolant, and impose the equation to hold at a set of collocation points. The new class of methods generalize the work of Gelbard and Seinfeld [13] to splines of arbitrary orders, and to any sequence of collocation points. The discretization approach is presented in the context of single component particle populations described by number densities; but it can be directly extended to mass or volume densities and multiple component particles.

The paper is organized as follows. Section 2 presents the particle dynamics equations and Section 3 surveys previous efforts to solve these equations numerically. A brief review of B-spline interpolation is given in Section 4. The new B-spline discretization approach is introduced in Section 5. Numerical results are presented in Section 6, and Section 7 draws conclusions and pinpoints future work.

2 The continuous particle dynamics equation

In this paper the continuous particle size distributions are considered functions of particle volume (v) and time (t). For simplicity we consider single component particles, but the discretization techniques can be directly generalized to multiple components. The size distribution function (number density) of a family of

particles will be denoted by $n(v,t)$; the number of particles per unit volume of air with the volume between v and $v+dv$ is $n(v,t)dv$. This describes completely a population of single-component particles. Similar formulations can be given in terms of volume, surface, or mass densities [24].

The aerosol population undergoes a series of physical and chemical transformations. *Growth* processes include condensation, evaporation, deposition and sublimation (of gases to/from the particle surface). The growth of each component's volume takes place at a rate that depends on the particle's dimension and composition, $dv/dt = I(v,t)$. *Coagulation* forms new particles of volume $v+w$ from the collision of two smaller particles of volumes v and w; the collision rate $\beta_{v,w} n(v) n(w)$ is proportional to the number of available small particles; the proportionality factor (called the coagulation kernel) is usually a symmetric function, $\beta_{v,w} = \beta_{w,v}$. *Nucleation* of gases creates small particles. *Emissions* increase the number of particles of a specific composition and size, while *deposition* processes remove particles from the atmosphere. In addition, the constituents interact chemically inside each particle, changing the chemical composition (but not the number) of particles. Under the above physical transformations the number density changes according to [12]

$$\begin{aligned} \frac{\partial n(v,t)}{\partial t} &= -\partial \left[I(v)\, n(v,t) \right] / \partial v \\ &\quad + \frac{1}{2} \int_{\text{initial}}^{v} \beta_{v-w,w}\, n(v-w,t) n(w,t) dw - n(v,t) \int_{\text{initial}}^{\infty} \beta_{v,w}\, n(w,t) dw \\ &\quad + S(v,t) - R(v,t)\, n(v,t) \ , \\ n(v,t=0) &= n^0(v) \ , \quad n(v=0,t) = 0 \ . \end{aligned} \tag{1}$$

The different terms in equation (1) describe, in order, the modification in the number of particles due to growth, creation of particles of volume v by coagulation, loss of volume v particles due to coagulation, increase in particle number due to sources (nucleation, emissions) and decrease due to depositions. The equation is subject to a specified initial condition $n^0(v)$, and to the boundary condition of no zero-volume particles.

In practice one assumes that the particle population has a nonzero minimal volume and a finite maximal volume, i.e. the dynamic equation is solved on a finite volume interval $[V_{\min}, V_{\max}]$.

$$\begin{aligned} \frac{\partial n(v,t)}{\partial t} &= -\partial \left[I(v)\, n(v,t) \right] / \partial v \\ &\quad + \frac{1}{2} \int_{V_{\min}}^{v-V_{\min}} \beta_{v-w,w}\, n(v-w,t) n(w,t) dw - n(v,t) \int_{V_{\min}}^{V_{\max}} \beta_{v,w}\, n(w,t) dw \\ &\quad + S(v,t) - R(v,t)\, n(v,t) \ , \\ n(v,t=0) &= n^0(v) \ , \quad n(V_{\min},t) = 0 \ . \end{aligned} \tag{2}$$

Note that this equation is no longer self-consistent; for $V_{\min} \le v < 2V_{\min}$ the upper integration limit is smaller than the lower integration limit in the positive coagulation term; we therefore introduce the convention that the positive coagulation term is zero whenever the upper limit is smaller than the lower integration limit.

Particle sizes span orders of magnitude, and to reveal the particle distribution logarithmic coordinates are popular. If we denote

$$x = \log v \ , \quad y = \log w \ , \quad X_{\min} = \log V_{\min} \ , \quad X_{\max} = \log V_{\max} \ ,$$

the dynamics equation becomes

$$\begin{aligned} \frac{\partial n(x,t)}{\partial t} &= -e^{-x} \partial \left[I(x)\, n(x,t) \right] / \partial x \\ &\quad + \frac{1}{2} \int_{X_{\min}}^{\log(e^x - e^{X_{\min}})} \beta_{\log(e^x - e^y),y}\, n(\log(e^x - e^y),t) n(y,t) e^y dy - n(x,t) \int_{X_{\min}}^{X_{\max}} \beta_{x,y}\, n(y,t) e^y dy \\ &\quad + S(x,t) - R(x,t)\, n(x,t) \ , \\ n(x,0) &= n^0(x) \ , \quad n(X_{\min},t) = 0 \ . \end{aligned} \tag{3}$$

3 Previous work

Three major approaches are used to represent the size distribution of aerosols: continuous, discrete and parameterized. In this paper we focus on continuous models (i.e. continuous size distributions and the general dynamic equations in continuous form).

For computational purposes one needs to use finite-dimensional approximations of the continuous size distributions. In the *sectional approach* the size domain $v \in [0, \infty]$ is divided into size bins $v \in [V_i^{\text{low}}, V_i^{\text{high}})$. In each size bin i there are α_i particles per unit volume, all of them having the same mean volume V_i. variations of this approach include the *full-moving* structure, the *quasi-stationary approach*, as well as the *moving-center* structure [17].

The integro-differential coagulation equation is difficult to solve accurately, due to the quadratic terms under the integral, as well as the Volterra nature of the first term. The algorithms proposed in the literature for the coagulation equation include semi-implicit solutions, finite element method, orthogonal collocation over finite elements, J-space transformations, analytical solutions [17, Section 16], [21] etc. A nice survey of several popular numerical methods for particle dynamics equations is given in Zhang et. al. [33].

Jacobson [17, Section 16] proposed the semi-implicit scheme to solve the discrete coagulation equation. In [27] we proposed a Newton-Cotes quadrature approach for solving the aerosol coagulation equation. Kim and Seinfeld [19] extended the moving sectional method to solve the multicomponent aerosol condensation equation. A nice survey of several popular numerical methods for the growth equations is given in Zhang et. al. [33]. In UAM-AERO and SAQM-AERO [20] the boundaries of the size sections move at a rate consistent with the growth rate equation (a Godunov-type advection scheme); CIT, UAM-AIM uses the Eulerian advection scheme of Bott [5]. In GATOR [16] the mean particle size in each bin i is allowed to grow. Jacobson [15] developed a highly complex gas, aerosol, transport and radiation model (GATOR). A combination of cubic splines (coagulation) and moving finite element techniques (growth part) was used by Tsang and Hippe [32]. Meng, Dabdub and Seinfeld [22] present a size-resolved and chemically-resolved model for aerosol dynamics in a mass density formulation. Different solution of the growth equations were proposed in [3, 16, 19, 20].

Pilinis [24] derived and solved the equations that govern the time evolution of mass distribution for a multicomponent particulate system using a Galerkin approach with linear basis functions. In [25] we proposed a general framework for the numerical treatment of aerosol dynamics that encompasses both Galerkin and collocation type methods; experiments were presented with higher order basis functions.

Gelbard and Seinfeld [12, 13, 14] solved the dynamic equations using a cubic spline approximation of the solution (in piecewise-polynomial form) and orthogonal collocation.

In this paper we generalize the Gelbard and Seinfeld approach [13]. We formulate the discretization in the general framework proposed in [25] using B-splines. This gives a broad class of discretization schemes based on spline interpolants of any order, and on any suitable choice of the collocation points.

4 B-Spline Interpolation

In this section we briefly review some basic aspects of B-spline interpolation. For more details the reader is invited to consult de Boor's monograph on the subject [4].

Consider a nondecreasing sequence of knots $K_1, \cdots, K_{s+k}$ with $K_1 \leq V_{\min}$, $K_{s+k} \geq V_{\max}$. The function $p(v)$ is a spline function of order k if it is a piecewise polynomial of degree at most $k-1$, i.e. $p(v)$ is a (different) polynomial of degree at most $k-1$ on each subinterval $[K_i, K_{i+1}]$. In addition, if the knots are simple (not repeated), then $p(v)$, $p'(v)$, $\cdots$, $p^{(k-2)}(v)$ are all continuous on the whole interval $[K_1, K_{k+s}]$. If a knot has multiplicity r, i.e. $K_i = K_{i+1} = \cdots = K_{i+r-1}$ then only $p(v)$, $p'(v)$, $\cdots$, $p^{(k-1-r)}(v)$ are continuous across that knot.

Any spline function can be expressed as a linear combination of the B-spline basis functions $\{\phi_i\}_{1 \leq i \leq s}$ associated with the given set of knots

$$p(v) = \sum_{i=1}^{s} \alpha_i \, \phi_i(v) \ . \tag{4}$$

Note that the dimension of the spline space is s (the number of knots minus k). Each B-spline has compact support (more exactly $\phi_i = 0$ outside the interval $[K_i, K_{i+k}]$) and takes values $0 \leq \phi_i(v) \leq 1$.

Let $n(v)$ be a smooth function on $v \in [V_{\min}, V_{\max}]$, and consider a set of s interpolation points $V_1, \cdots, V_s$ in this interval. There is a unique spline function that interpolates n at the given points:

$$p(V_j) = n(V_j) \ , \quad j = 1 \cdots s \ .$$

The s interpolation conditions can be written as

$$A \ [\alpha_1, \cdots, \alpha_s]^T = [n(V_1), \cdots, n(V_s)]^T \tag{5}$$

where the B-spline basis collocation matrix is

$$A = [\phi_j(V_i)]_{1 \le i,j \le s} \ . \tag{6}$$

Note that the knots and interpolation points must be chosen such that A is nonsingular. Similarly, the function derivative is approximated by the derivative of the spline interpolant

$$n'(v) \approx p'(v) = \sum_{i=1}^{s} \alpha_i \, \phi_i'(v) \ . \tag{7}$$

At the interpolation points this becomes

$$[n'(V_1), \cdots, n'(V_s)]^T \approx D \ [\alpha_1, \cdots, \alpha_s]^T \ ,$$

where the B-spline basis derivative collocation matrix is

$$D = \left[\phi_j'(V_i)\right]_{1 \le i,j \le s} \ . \tag{8}$$

Accuracy of spline polynomial interpolation. We recall the following result from [4] which shows how well do the spline interpolant and its derivatives approximate the function and its derivatives. If $n(v)$ is smooth then

$$\max_{V_{\min} \le v \le V_{\max}} |n^{(j)}(v) - p^{(j)}(v)| \le C_j \, |h|^{k-j} \max_{V_{\min} \le v \le V_{\max}} |n^{(k)}(v)| \ , \quad h = \max_j |V_{j+1} - V_j| \ . \tag{9}$$

Choosing the knots and the interpolation points. Clearly there are many possible choices of knots and interpolation points, each defining a different aerosol discretization method. Note that we will use the interpolation points as collocation points in formulating the discretized particle dynamics equations.

In this paper we consider the set of s Chebyshev interpolation points in the interval $[V_{\min}, V_{\max}]$ (cf. [31]) which leads to a non-oscillatory interpolant

$$V_j = V_{\min} + \frac{V_{\max} - V_{\min}}{2} \left[1 - \cos\left(\frac{j-1}{s-1}\pi\right)\right] \ , \quad j = 1 \cdots s \ . \tag{10}$$

We use the Schoenberg knots associated with the Chebyshev interpolation points for the construction of B-spline basis

$$\begin{array}{rcll} K_i & = & V_1 \ , & i = 1, \cdots, k \\ K_{k+i} & = & \left(\sum_{j=i+1}^{i+k-1} V_j\right) / (k-1) \ , & i = 1, \cdots, s-k \\ K_i & = & V_s \ , & i = s+1, \cdots, s+k \end{array} \tag{11}$$

Note that the Gelbard and Seinfeld approach [13] corresponds to $k = 4$ (cubic splines); there are $2M + 4$ knots, taking M distinct and equidistant values (all interior knots are double, while the first and the last knot have multiplicity 4); finally, there are $2M$ collocation points at the roots of the shifted Legendre polynomial (3 points in the first and in the last knot intervals, and 2 collocation points in each of the other knot intervals).

The Gelbard and Seinfeld approach ("orthogonal collocation over finite elements") can be generalized to splines of arbitrary even order k as follows. The number of degrees of freedom (number of collocation points) is $s = M(k/2)$, where M is the number of distinct knot values. The first and the last knots have multiplicity k, and all the interior knots have multiplicity $k/2$. In each knot interval i $(1 \le i \le M - 1)$

we place $k/2 + n_i$ collocation points at the zeros of the shifted Legendre polynomial (i.e. Gauss quadrature points in the knot interval). The extra points n_i are chosen such that $n_1 + \cdots + n_{M-1} = k/2$, and $n_1 \geq 1$ (since we need one collocation point to impose the boundary condition). Our numerical experiments showed this orthogonal collocation over finite elements approach to be less accurate than the Chebyshev collocation (with Schoenberg knots) approach.

Similarly, the finite element basis we used in [25] corresponds to equispaced knots of multiplicity $k-1$ for different k-s; the collocation points are the knots, plus $k-1$ equispaced points inside each knot interval.

Logarithmic coordinates. In the logarithmic formulation (3) the knots K_i and the collocation points X_i are chosen similarly in the interval $[X_{\min}, X_{\max}]$. The B-spline basis functions are constructed in the variable $x = \log v$, which gives the collocation matrices

$$A = [\phi_j(X_i)]_{1 \leq i,j \leq s} \ , \qquad D = \left[\phi_j'(X_i)\right]_{1 \leq i,j \leq s} \ .$$

5 The discrete formulation of aerosol dynamics

Following the general approach we developed in [25], the equation (1) is solved by a semi-discretization in particle size (v) plus a time integration of the resulting system of ordinary differential equations. The semi-discretization in size is done by approximating the solution with the B-spline polynomial interpolant, (i.e. projecting the solution and the equation on the finite-dimensional subspace spanned by B-spline basis functions $\{\phi_1, \cdots, \phi_s\}$) and by imposing the resulting equation to hold exactly at the set of collocation points. Here we present the derivation only briefly; for more details the reader is invited to consult [25]. For simplicity single-component particle populations described completely by the number density are considered; but the ideas can be directly extended to multiple (mass or volume) distributions for multiple-component aerosols.

5.1 Discretization of the particle size distribution

From (4) one can approximate the continuous particle distribution by the B-spline interpolation polynomial

$$n(v,t) = \sum_{i=1}^{s} \alpha_i(t)\, \phi_i(v) \ , \tag{12}$$

The approximation is finite dimensional, with the set of time-dependent B-spline coefficients

$$\alpha(t) = [\, \alpha_1(t), \cdots, \alpha_s(t) \,]^T \ , \tag{13}$$

to be determined from the dynamics equation.

Let $\{V_j\}_{1 \leq j \leq s}$ be a set of collocation points. The interpolation condition gives the coefficients α as a solution of the linear system:

$$A\, \alpha(t) = [\, n(V_1,t), \cdots, n(V_s,t) \,]^T \ .$$

In the logarithmic formulation

$$A\, \alpha(t) = [\, n(X_1,t), \cdots, n(X_s,t) \,]^T \ .$$

5.2 Coagulation

The theoretical coagulation equation for single-component particles is [17, Section 16]

$$\frac{\partial n(v,t)}{\partial t} = \frac{1}{2} \int_{V_{\min}}^{v - V_{\min}} \beta_{v-w,w}\, n(v-w,t) n(w,t) dw - n(v,t) \int_{V_{\min}}^{V_{\max}} \beta_{v,w}\, n(w,t) dw \ . \tag{14}$$

To obtain a discrete form of the coagulation equation one inserts the B-spline polynomial approximation (12) into (14), and imposes the resulting equation to hold exactly at the set of collocation points V_j, $1 \leq j \leq s$.

After some calculations (see [25]) one arrives at

$$A\,\alpha'(t) = \begin{bmatrix} \alpha^T(t)\ \left(B^1 - C^1\right)\ \alpha(t) \\ \vdots \\ \alpha^T(t)\ \left(B^s - C^s\right)\ \alpha(t) \end{bmatrix}\ , \tag{15}$$

with the matrices

$$\begin{array}{rcl} B^j & = & \left[(1/2)\int_{V_{\min}}^{V_j - V_{\min}} \beta_{V_j - w, w}\phi_k(V_j - w)\phi_m(w)dw\right]_{1\le k,m\le s}\ , \quad 1 \le j \le s\ , \\ C^j & = & \left[\phi_k(V_j)\int_{V_{\min}}^{V_{\max}} \beta_{V_j, w}\phi_m(w)dw\right]_{1\le k,m\le s}\ , \quad 1 \le j \le s. \end{array} \tag{16}$$

One can regard B and C as three-tensors and compactly write the discrete equation (15) as

$$A\,\alpha'(t) = \left[(B - C) \times \alpha(t)\right] \cdot \alpha(t). \tag{17}$$

The discrete coagulation system is bilinear. The Jacobian of the coagulation term can be expressed as

$$J^{\mathrm{coag}}(\alpha) = \begin{bmatrix} \alpha^T \left\{(B^1 - C^1) + (B^1 - C^1)^T\right\} \\ \vdots \\ \alpha^T\ \left\{(B^s - C^s) + (B^s - C^s)^T\right\} \end{bmatrix}\ .$$

Particularly attractive are linearly implicit time-stepping methods which preserve stability yet avoid iterative solutions. For example, the linearized backward Euler scheme reads

$$\left(A - \frac{\Delta t}{2} J^{\mathrm{coag}}(\alpha^k)\right)\ \alpha^{k+1} = \alpha^k\ . \tag{18}$$

Here α^k, α^{k+1} denote the numerical approximations of $\alpha(t^k)$ and $\alpha(t^{k+1})$, with the time moments related by $t^{k+1} = t^k + \Delta t$.

In the logarithmic formulation (3) one defines the coagulation tensors as

$$\begin{array}{rcl} B^j & = & \left[(1/2)\int_{X_{\min}}^{\log(e^{X_j} - e^{X_{\min}})} \beta_{\log(e^{X_j} - e^y), y}\phi_k(\log(e^{X_j} - e^y))\phi_m(y)e^y dy\right]_{1\le k,m\le s}\ , \quad 1 \le j \le s\ , \\ C^j & = & \left[\phi_k(X_j)\int_{X_{\min}}^{X_{\max}} \beta_{X_j, y}\phi_m(y)e^y dy\right]_{1\le k,m\le s}\ , \quad 1 \le j \le s. \end{array} \tag{19}$$

Note that one similar formulas are derived for a Galerkin formulation; the tensor entries in this case involve double integrations.

5.3 Growth

The growth equation in number densities

$$\frac{\partial n(v,t)}{\partial t} = -\frac{\partial}{\partial v}\left[I(v)\,n(v,t)\right]\ , \quad I(v) = \frac{dv(t)}{dt}\ , \quad n(v=0,t) = 0\ , \quad n(v,t=0) = n^0(v)\ , \tag{20}$$

has the form of an advection equation, with the "flow speed" provided by the growth rate $I(v)$ (i.e. the time derivative of the particle volume). This equation is to be solved subject to an initial distribution $n^0(v)$ and the boundary condition of no zero-sized particles [28, Section 12],

To obtain a discrete version of the growth equation we need to either interpolate the flux $I(v)n(v,t)$ or to explicitly use the derivative of the growth rate in

$$\frac{\partial n(v,t)}{\partial t} = -\frac{\partial}{\partial v}\left[I(v)\,n(v,t)\right] = -\frac{\partial I}{\partial v}(v)\,n(v,t) - I(v)\frac{\partial n}{\partial v}(v,t) \tag{21}$$

We take the (practical) approach of interpolating the growth rate and approximating its derivative by the derivative of the interpolant:

$$I(v) = \sum_{i=1}^{s} \gamma_i\,\phi_i(v)\ , \qquad \gamma = \left[\gamma_1, \cdots, \gamma_s\right]^T\ , \qquad A\,\gamma = \left[I(V_1), \cdots, I(V_s)\right]^T$$

and therefore

$$[\,\partial I/\partial v(V_1),\cdots,\partial I/\partial v(V_s)\,]^T \approx D\gamma\ .$$

The growth equation (21) is imposed to hold exactly at the collocation points

$$\begin{aligned}
\begin{bmatrix} n'(V_1,t) \\ \vdots \\ n'(V_s,t) \end{bmatrix} &= -\begin{bmatrix} \partial I/\partial v(V_1)\cdot n(V_1,t) \\ \vdots \\ \partial I/\partial v(V_s)\cdot n(V_s,t) \end{bmatrix} - \begin{bmatrix} I(V_1)\cdot \partial n/\partial v(V_1,t) \\ \vdots \\ I(V_s)\cdot \partial n/\partial v(V_s,t) \end{bmatrix} \\
&= -\mathrm{diag}_j\left[\frac{\partial I}{\partial v}(V_j)\right]\cdot\begin{bmatrix} n(V_j,t) \\ \vdots \\ n(V_j,t) \end{bmatrix} - \mathrm{diag}_j\,[I(V_j)]\cdot\begin{bmatrix} \partial n/\partial v(V_1,t) \\ \vdots \\ \partial n/\partial v(V_s,t) \end{bmatrix} \\
&\approx -\mathrm{diag}\,[\,D\gamma\,]\;A\,\alpha(t) - \mathrm{diag}\,[\,A\gamma\,]\;D\,\alpha(t)
\end{aligned}$$

Therefore the growth equation expressed in the B-spline coefficients is

$$A\,\alpha'(t) = -G\,\alpha(t) \quad \text{where} \quad G = \mathrm{diag}\,[\,D\gamma\,]\cdot A + \mathrm{diag}\,[\,A\gamma\,]\cdot D. \tag{22}$$

To impose the boundary condition at $v = V_{\min}$ we always let $V_1 = V_{\min}$. The boundary condition can be written in terms of the first row of matrix A

$$n(V_{\min},t) = n(V_1,t) = g(t) \quad \Leftrightarrow \quad \sum_{i=1}^{s}\alpha_i\phi_i(V_1) = A_{1,1:s}\,\alpha(t) = g(t)\ . \tag{23}$$

Therefore we impose the equation (22) to hold at V_2 through V_s and the boundary condition (23) to hold at V_1. For example, if a trapezoidal time discretization is used the discrete system (22)–(23) reads

$$\left(A + \frac{\Delta t}{2}\begin{bmatrix} 0_{1:s}^T \\ G_{2:s,1:s} \end{bmatrix}\right)\alpha^{k+1} = \begin{bmatrix} g(t^{k+1}) \\ \left(A_{2:s,1:s} - \frac{\Delta t}{2}G_{2:s,1:s}\right)\alpha^k \end{bmatrix}\ .$$

In the logarithmic formulation (3) the growth equation reads

$$\frac{\partial n(x,t)}{\partial t} = -e^{-x}\frac{\partial\,[I(x)\,n(x,t)]}{\partial x}\ , \quad I(x) = e^x\frac{dx(t)}{dt}\ , \quad n(X_{\min},t) = 0\ , \quad n(x,0) = n^0(x)\ . \tag{24}$$

The logarithmic semidiscrete growth equation is of the form (22), with γ defined in logarithmic coordinates and with

$$G = \mathrm{diag}_j\,[e^{-X_j}]\cdot(\mathrm{diag}\,[\,D\gamma\,]\cdot A + \mathrm{diag}\,[\,A\gamma\,]\cdot D)\ .$$

Note that the growth equation (20) has the form of an advection equation; spurious oscillations in the numerical solution may appear when a nonsmooth distribution is subject to strong growth (advection). Total variation diminishing (TVD) advection schemes are used to suppress spurious oscillations. The use of such schemes for aerosol growth calculations was advocated by Dabdub and co-workers[7, 8]. For a comprehensive treatment of non-oscillatory advection methods see [10].

It is possible to construct total variation diminishing advection schemes using the the B-spline interpolant as follows. We regard n_i as the mean number concentration in size bin i; this size bin contains particles with volumes in between $V_{i-1/2}$ and $V_{i+1/2}$, where the bin boundaries are

$$V_{i+1/2} = \frac{V_i + V_{i+1}}{2}\ , \quad 1 \le i \le s-1\ .$$

The growth equation (20) can be written in conservative (flux) form as

$$n_i^{k+1} = n_i^k + \frac{\Delta t}{V_{i+1/2} - V_{i-1/2}}\left(f_{i-1/2}^k - f_{i+1/2}^k\right)\ . \tag{25}$$

The bin boundary number density values can be obtained by B-spline interpolation

$$\begin{bmatrix} n^k(V_{1/2}) \\ \vdots \\ n^k(V_{s-1/2}) \end{bmatrix} = A_F\,\alpha^k\ , \qquad A_F = \left(\phi_j(V_{i+1/2})\right)_{1\le i\le s-1,1\le j\le s}\ ,$$

which gives a high order approximation of the inter-bin fluxes

$$f^{\text{high}}_{i+1/2} = I(V_{i+1/2})\, n(V_{i+1/2}).$$

The first order upwind scheme is monotonic; this scheme uses a low order approximation of the flux,

$$f^{\text{low}}_{i+1/2} = I(V_{i+1/2})\, n_i.$$

A total variation diminishing scheme is obtained by limiting the high-order flux to the low-order flux in regions of sharp gradients [10, Section 5]

$$f_{i+1/2} = f^{\text{low}}_{i+1/2} + L(r_{i+1/2}) \left(f^{\text{high}}_{i+1/2} - f^{\text{low}}_{i+1/2} \right) , \qquad r_{i+1/2} = \frac{n_i - n_{i-1}}{n_{i+1} - n_i}.$$

There are numerous suitable limiters L; an example is the superbee function [10, Section 5]

$$L(r) = \max\left(0, \min(1, 2r), \min(2, r)\right) \ .$$

With F the vector of limited inter-bin fluxes, and with ΔV, ΔF denoting the bin size and flux difference vectors respectively, the equation (25) becomes

$$A\,\alpha^{k+1} = A\,\alpha^k + \Delta t \cdot \mathrm{diag}\,[\Delta V] \cdot \Delta F(\alpha^k) \ .$$

5.4 Sources and sinks

Sources (emissions, nucleation) and sinks (removal processes) have a simple mathematical formulation,

$$\frac{\partial n(v,t)}{\partial t} = S(v,t) - R(v,t)\, n(v,t) \ .$$

The simplicity comes from the fact that the S and R terms are not coupled across different volumes. Using the spline interpolant (12) in place of n and imposing the resulting equation to hold at the collocation points leads to

$$A\,\alpha'(t) = S(t) - R(t)\, A\,\alpha(t) \ , \tag{26}$$

with

$$S(t) = \left[\, S(V_1,t), \cdots, S(V_s,t) \,\right]^T \ , \quad R(t) = \mathrm{diag}\left[\, R(V_1,t), \cdots, R(V_s,t) \,\right] \ .$$

A trapezoidal (Crank-Nicholson) integration of (26) gives

$$\left(A + \frac{\Delta t}{2} R^{k+1} A \right) \alpha^{k+1} = \left(A - \frac{\Delta t}{2} R^k A \right) \alpha^k + \Delta t\, S^{k+\frac{1}{2}} \ ,$$

where

$$S^{k+\frac{1}{2}} = \frac{S^k + S^{k+1}}{2} \ .$$

In the logarithmic formulation (3) one defines

$$S(t) = \left[\, S(X_1,t), \cdots, S(X_s,t) \,\right]^T \ , \quad R(t) = \mathrm{diag}\left[\, R(X_1,t), \cdots, R(X_s,t) \,\right] \ .$$

5.5 Simultaneous discretization of the dynamic equations

A coupled solution of coagulation, growth, nucleation, emissions and deposition is of interest; it will, for example, better capture the competition between nucleation of new particles and condensation on existing particles for gas-to-particle conversion [33].

For single component particles combining (15), (22) and (26) gives the semi-discrete aerosol dynamics equation

$$A\,\alpha'(t) = \underbrace{-G\,\alpha(t)}_{\text{growth}} + \underbrace{\left[(B-C) \times \alpha(t)\right] \alpha(t)}_{\text{coagulation}} + \underbrace{S(t)}_{\text{nucl.+em}} \underbrace{-R\,A\,\alpha(t)}_{\text{dep.}} \ . \tag{27}$$

This is a system of s coupled ordinary differential equations. The discrete initial conditions are obtained from the interpolation of the initial condition

$$\alpha(0) = [\, \alpha_1^0, \cdots, \alpha_s^0 \,]^T \quad , \quad n^0(v) = \sum_{i=1}^{s} \alpha_i^0 \phi_i(v) \; . \tag{28}$$

The system (27)-(28) can be solved by any appropriate time-stepping method. The system has a particular form: the growth term is linear, while the coagulation term is bilinear. Combining the linearized backward Euler scheme for coagulation with Crank-Nicholson for growth and sources/sinks we achieve second order time accuracy:

$$\left(A - \frac{\Delta t}{2} \left\{ J^{\mathrm{coag}}(\alpha^k) - (G + R^{k+1} A) \right\} \right) \alpha^{k+1} = \left(A - \frac{\Delta t}{2} (G + R^k A) \right) \alpha^k + \Delta t \, S^{k+\frac{1}{2}} \; . \tag{29}$$

Like before superscripts denote the discrete times at which the entities are evaluated. Imposing the left boundary condition can be done by replacing the first equation in (29) with (23)

$$\left(A - \frac{\Delta t}{2} \begin{bmatrix} 0_{1:s}^T \\ \left\{ J^{\mathrm{coag}}(\alpha^k) - (G + R^{k+1} A) \right\}_{2:s,1:s} \end{bmatrix} \right) \alpha^{k+1} = \begin{bmatrix} g(t^{k+1}) \\ \left\{ \left(A - \frac{\Delta t}{2} (G + R^k A) \right) \alpha^k + \Delta t S^{k+\frac{1}{2}} \right\}_{2:s,1:s} \end{bmatrix} . \tag{30}$$

At each step the number concentration vector can be easily retrieved

$$n^k = A \, \alpha^k \; .$$

6 Numerical experiments

Problem A. For the numerical experiments we first consider the test problem from [13], which admits an analytical solution. Let N_{t} be the total initial number of particles and V_{m} the mean initial volume. The initial number distribution is exponential, the coagulation rate is constant, and the growth rate is linear with the volume:

$$N_{\mathrm{t}}(v) = (N_{\mathrm{t}}/V_{\mathrm{m}}) \, e^{-v/V_{\mathrm{m}}} \; , \quad \beta(v,w) = \beta_0 \; , \quad I(v) = \sigma_o \, v \; .$$

The analytical solution (see [13]) is

$$n^A(v,t) = \frac{4 N_{\mathrm{t}}}{V_{\mathrm{m}} (N_{\mathrm{t}} \beta_o t + 2)^2} \cdot \exp\left(\frac{-2v \exp(\sigma_o t)}{V_{\mathrm{m}} (N_{\mathrm{t}} \beta_o t + 2)} - \sigma_o t \right) \; .$$

We solve the dynamics equation for $\beta_o = 6.017 \times 10^{-10}$ cm^{3}sec^{-1}particles^{-1}, $\sigma_o = 0.03$ hour^{-1}, $N_{\mathrm{t}} = 10^4$ particles, $V_{\mathrm{m}} = 0.03$ μm^3. The value of σ_o is chosen such that coagulation and growth have effects of comparable magnitude.

The equation was solved on the time interval $[\, t_{\mathrm{initial}} = 0, \; t_{\mathrm{final}} = 6 \text{ hours} \,]$ with a small time step $\Delta t =$ 1 second; the timestep was chosen such that the time discretization errors are small compared to the size discretization errors. The volume interval $[\, V_{\min} = \pi/6 \times 10^{-9} \; \mu\mathrm{m}^3, \; V_{\max} = \pi/6 \; \mu\mathrm{m}^3 \,]$ corresponds to a particle diameter range $[\, D_{\min} = 10^{-3} \; \mu\mathrm{m}, \; D_{\max} = 1 \; \mu\mathrm{m} \,]$.

Problem B. The second test problem is posed naturally in logarithmic coordinates; the initial concentration is a (logarithmic) cosine hill

$$n_0(v) = \begin{cases} \frac{N_{\mathrm{t}}}{2} \cdot \left[1 - \cos\left(2\pi \frac{\log v - x_{\min}}{x_{\max} - x_{\min}} \right) \right] \; , & \log V_{\min} < x_{\min} < \log v < x_{\max} < \log V_{\max} \; . \\ 0 \; , & \log v \le x_{\min} \text{ or } \log v \ge x_{\max} \; . \end{cases}$$

The parameter values used are $\beta_o = 1.083 \times 10^{-3}$ cm^3 hour^{-1} particles^{-1}, $I(v) = 0.02$ μm^{3}hour^{-1} = const, and $N_{\mathrm{t}} = 10^4$ particles. The volume interval is $[\, V_{\min} = 10^{-3} \, \mu\mathrm{m}^3, \; V_{\max} = 1 \, \mu\mathrm{m}^3 \,]$, the time interval $[\, t_{\mathrm{initial}} = 0, \; t_{\mathrm{final}} = 1 \text{ hour} \,]$, and the time step $\Delta t = 1$ second.

The reference solution was obtained using the standard numerical method for coagulation [17] on the uniform grid $V_i = i \cdot \Delta v$, $\Delta v = 10^{-4}\ \mu m^3$, such that $V_1 = V_{\min}$ and $V_{10,000} = V_{\max}$. The reference growth-coagulation solution is obtained by translating the reference coagulation solution 200 gridpoints to the right.

Problem B is a challenging test due to two factors. First, the initial distribution is continuously differentiable, but its second derivative is not continuous. We expect that the accuracy of the spline approximations is affected by the limited smoothness of this test problem; specifically, the error bound (9) will only hold for $k < 2$ regardless of the spline interpolant order. Second, the growth rate is the same for all particle sizes. In the classical Fuchs and Sutugin approach [11] the growth rate is approximately of the form $I(v) \approx \sigma\, v^{2/3}$; i.e. the smaller the particle the smaller its growth rate. With problem B the growth rate is large for small particle sizes too (i.e. at and near the inflow boundary); due to the logarithmic distribution of discretization points the CFL number can become very large in the small particle range.

Error Measure. The accuracy of the numerical solutions at the final time is measured against the analytical (or reference) solution by the root-mean-square (RMS) error norm

$$\|E\| = \sqrt{\frac{1}{s}\sum_{i=1}^{s}\left(\frac{n\left(V_i, t_{\text{final}}\right) - n^A\left(V_i, t_{\text{final}}\right)}{\max(n^A\left(V_i, t_{\text{final}}\right), th)}\right)}\,. \tag{31}$$

The threshold $th = 1000\ \text{particles}\,\text{cm}^{-3}\,\mu\text{m}^{-3}$ makes the error indicator to ignore the smallest part of the number distribution. The use of a finite volume interval for problem A introduces errors in the coagulation right-hand-side of the order of 10^{-8}. The best accuracy we can hope for is consequently of this magnitude regardless of how many size bins we use.

Experiment I. In this experiment we solve test problem A in the formulation (2), i.e. in linear volume coordinate. We consider separately the coagulation-only and growth-only problems in addition to coagulation and growth. Figure 1 plots the error norm of the solution at the end of the simulation time versus the number of bins; the errors decrease rapidly. The accuracy of coagulation is bounded below at 10^{-8} due to the finite volume interval approximation. For $s = 10$ the exact solutions are reproduced within acceptable "visual accuracy" for all tests; this means that the plot of the numerical solution nearly overlaps the plot of the exact solution. For larger numbers of bins the errors decrease rapidly, and the slopes of the error curves illustrate the convergence orders of different methods. The slopes, i.e. the experimental convergence orders, are given in Table 1; for all tests the convergence orders are better than the spline order k, which suggests a superconvergence phenomenon.

Experiment II. We now solve the test problem A in the logarithmic formulation (3). The approach uses B-spline interpolation in the $x = \log v$ variable. The resulting solution accuracies are shown in Figure 2; for the same number of bins the solutions are slightly less accurate in logarithmic than in linear coordinates. Growth errors show a lower bound of about 10^{-6} which may indicate the existence of another source of numerical errors, that becomes more important than the discretization errors at large values of s. The experimental orders of convergence (outside the lower plateau) are shown in Table 1 and they agree well with our expectations. From a practical perspective, acceptable "visual accuracy" can be obtained with 10 to 20 bins.

Experiment III. For this experiment we solve the test problem B in logarithmic coordinates. Figure 3 shows the results. The experimental convergence orders (shown in Table 1) are limited by the smoothness of the test problem. Figure 4 shows the numerical solution for quintic splines (k=6) and 12 bins. The "visual accuracy" of the numerical solution is satisfactory. The numerical solution shows some small but spurious oscillations upwind of the concentration profile.

Wiggles appear when a nonsmooth distribution is subject to strong growth; total variation diminishing advection schemes can suppress these spurious oscillations at the price of some accuracy loss in areas of sharp gradients. For the purpose of comparison, Figure 5 presents the growth solutions obtained with the total variation diminishing method presented in Section 5.3; the low-order fluxes are given by the first

order upwind formula, the high-order corrective fluxes at intercell boundaries are obtained by B-spline interpolation, and a superbee limiter is used. Log-Chebyshev and log-uniform distributions of collocation points are considered, both with the Schoenberg placement of knots. The flux limited solutions are monotonic (no spurious oscillations) but the distribution peak is smeared. The log-uniform solution is more accurate.

7 Conclusions and Future Work

Simulation of aerosols plays a significant role in air pollution modeling. For a correct representation of particles in the atmosphere one needs to accurately solve for the size distribution of particle populations.

In this work we developed a family of discretization methods for the aerosol dynamics equation based on approximating the solution by a B-spline polynomial interpolant and collocating the equation. Different methods are obtained by choosing different B-spline bases, i.e. by selecting the B-spline order, the knots and the collocation points. The resulting semidiscrete system is bilinear (due to coagulation terms) and can be solved by the time stepping method of choice. The present formulation of the discretization method is based on number densities and single-component particles. The same discretization technique can be easily and directly applied to volume, surface and mass densities, as well as to multiple densities that model multiple-component aerosols.

The performance of the methods is illustrated on two test problems: one is smooth, involves an exponential distribution in the infinite volume range $v \in [0, \infty]$, and admits an analytical solution; the second one involves a finitely-supported cosine hill distribution and is formulated in logarithmic coordinates. The accuracy of solutions for the smooth problem improves rapidly with increased number of bins in both linear and logarithmic coordinates; the convergence orders depend on the order of the B-spline interpolant. The convergence orders for the cosine hill problem are limited by the limited smoothness of the profile. Nevertheless, for both problems, good solutions are obtained with a small number of bins. The cosine hill growth solution displays small but spurious oscillations; they can be eliminated by using a flux-limited advection scheme for which the high order inter-cell fluxes are obtained by B-spline interpolation.

Future work will focus on testing the B-spline discretization method on real-life problems involving the coagulation, growth and nucleation of particles under clear and hazy conditions. The method will be extended to multiple component particles and to coupled aerosol dynamics and chemistry systems. Attention will be paid to the use of non-oscillatory yet non-dissipative discretization schemes for the growth equation.

Acknowledgments

This work was supported by NSF through CAREER award no. ACI-0093139.

References

[1] K.E. Atkinson. *An Introduction to Numerical Analysis.* John Wiley and Sons, 1988.

[2] K.E. Atkinson. *The Numerical Solution of Integral Equations of the Second Kind.* Cambridge University Press, 1997.

[3] F.S. Binkowski and U. Shankar. The regional particulate matter model: 1: model description and preliminary results. *Journal of Geophysical research*, 100:26,191–26,209, 1995.

[4] C. de Boor. A practical guide to splines. *Springer-Verlag, New York*, 1978.

[5] A. Bott. A positive definite advection scheme obtained by nonlinear renormalization of the advection fluxes. *Monthly Weather Review*, 117:1006–1115, 1989.

[6] V. Ramanathan, P.J. Crutzen, M.O. Andreae, J. Coakley, R. Dickerson, J. Heintzenberg, A. Heymsfield, J.T. Kiehl, D. Kley, T.N. Krishnamurti, J. Kuettner, J. Lelieveld, S.C. Liu, A.P. Mitra, J. Prospero, R. Sadourny, A.F. Tuck, and F.P.J. Valero. Indoex white paper. Indian Ocean Experiment, http://www-indoex.ucsd.edu/publications/white_paper, 1998.

[7] K. Nguyen and D. Dabdub Two-level time-marching scheme using splines for solving the advection equation. Atmospheric Environment 35, (2001) 1627-1637.

[8] K. Nguyen and D. Dabdub Semi-Lagrangian flux scheme for the solution of the aerosol condensation/evaporation equation. Aerosol Science & Technology. Accepted, 2001.

[9] L.M. Delves and J.L. Mohamed. *Computational methods for integral equations.* Cambridge University Press, 1985.

[10] D.R. Duran. *Numerical Methods for Wave Equations in Geophysical Fluid Dynamics.* Springer Verlag New-York, Berlin, Heidelberg, 1998.

[11] N.A. Fuchs and A.G. Sutugin. High dispersed aerosols. *Topics in Current Aerosol Research*, G.M. Hidy and J.R. Brock editors, 1–60, 1971.

[12] F.M. Gelbard and J.H. Seinfeld. Coagulation and growth of a multicomponent aerosol. *Journal of Colloid and Interface Science*, 63(3):472–479, 1978.

[13] F.M. Gelbard and J.H. Seinfeld. Numerical solution of the dynamic equation for particulate systems. *Journal of Computational Physics*, 28:357–375, 1978.

[14] F.M. Gelbard and J.H. Seinfeld. Simulation of multicomponent aerosol dynamics. *Journal of Colloid and Interface Science*, 78(2):485–501, 1980.

[15] M.Z. Jacobson. Development and application of a new air pollution modeling system - II. Aerosol module structure and design. *Atmospheric Environment*, 31(2):131–144, 1997.

[16] M.Z. Jacobson. Numerical techniques to solve condensational and dissolutional growth equations when growth is coupled to reversible reactions. *Aerosol Science and Technology*, 27:491–498, 1997.

[17] M.Z. Jacobson. *Fundamentals of atmospheric modeling.* Cambridge University Press, 1999.

[18] C. Johnson. *Numerical Solution of Partial Differential Equations by the Finite Element Method.* Cambridge University Press, 1987.

[19] Y.P. Kim and J.H. Seinfeld. Simulation of multicomponent aerosol condensation by the moving sectional method. *Journal of Colloid and Interface Science*, 135(1):185–199, 1990.

[20] F.W. Lurmann, A.S. Wexler, S.N. Pandis, S. Musara, N. Kumar, and J.H. Seinfeld. Modeling urban and regional aerosols - ii. application to California's south coast air basin. *Atmospheric Environment*, 31:2695–2715, 1997.

[21] A.A. Lushnikov. Evolution of coagulating systems iii. coagulating mixtures. *Journal of Colloid and Interface Science*, 54(1):94–101, 1976.

[22] Z. Meng, D. Dabdub, and J.H. Seinfeld. Size-resolved and chemically resolved model of atmospheric aerosol dynamics. *Journal of Geophysical Research*, 103(D3):3419–3435, 1998.

[23] M. Phadnis and G.R. Carmichael. Transport and distribution of primary and secondary non-methane hydrocarbons in east Asia under continental outflow conditions. *J. Geophys. Res.*, in press, 1999.

[24] C. Pilinis. Derivation and numerical solution of the species mass distribution equation for multicomponent particulate systems. *Atmospheric Environment*, 24A(7):1923–1928, 1990.

[25] A. Sandu and C. T. Borden. A Framework for the Numerical Treatment of Aerosol Dynamics Technical Report CSTR-01-03, Department of Computer Science, Michigan Technological University, 1400 Townsend Drive, Houghton, MI 49931, 2001.

[26] A. Sandu. A Spectral Method for Solving Aerosol Dynamics Technical Report CSTR-01-04, Department of Computer Science, Michigan Technological University, 1400 Townsend Drive, Houghton, MI 49931, 2001.

[27] A. Sandu. A Newton-Cotes Quadrature Approach for Solving the Aerosol Coagulation Equation *Atmospheric Environment*, accepted, 2001.

[28] J.H. Seinfeld and S.N. Pandis. *Atmospheric chemistry and physics. From air pollution to climate change.* John Wiley & Sons, Inc., 1997.

[29] C.H. Song and G.R. Carmichael. Partitioning of hno3 modulated by alkaline aerosol particles. *J. Geophys. Res.*, in review, 1999.

[30] C.H. Song, G.R. Carmichael, and S.Y. Cho. An alternative way to couple kinetic (non-equilibrium/condensation/evaporation process with thermodynamic equilibrium relationships. *Atmospheric Environment*, to be submitted, 1999.

[31] L.N. Trefethen. Spectral methods in Matlab. SIAM Software, Environments, Tools Series, 2000.

[32] H. Tsang and J.M. Hippe. Asymptotic behavior of aerosol growth in the free molecule regime. *Aerosol Science and Technology*, 8:265–278, 1988.

[33] Y. Zhang, J.H. Seinfeld, M.Z. Jacobson, and F.S. Binkowski. Simulation of aerosol dynamics: a comparative review of algorithms used in air quality models. *Aerosol Science and Technology*, 31:487–514, 1999.

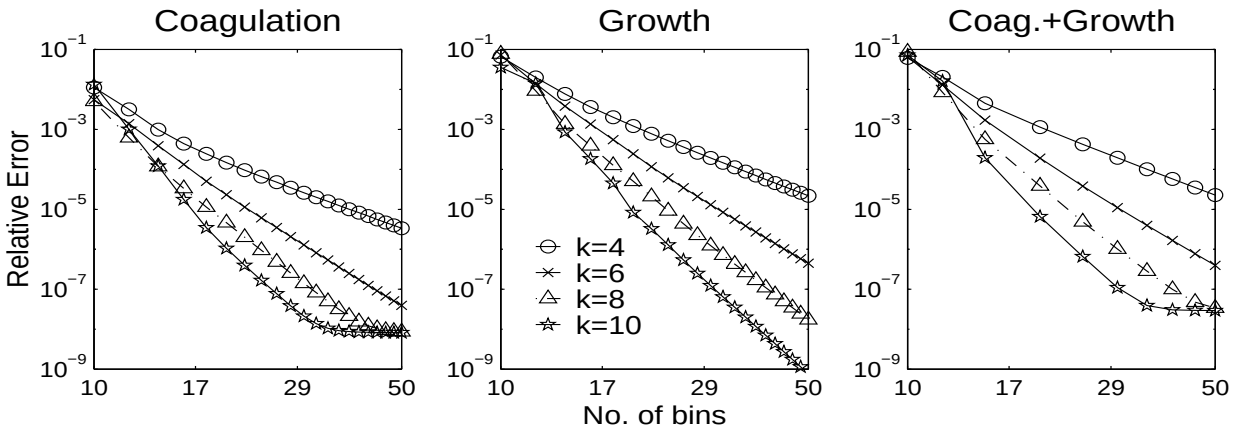

Figure 1: Experiment I (problem A in linear coordinates). Accuracy of final solutions ($t_{\text{final}} = 6$ hours) versus the number of bins for coagulation only, growth only, and coagulation-growth problems. Spline bases of different orders are considered.

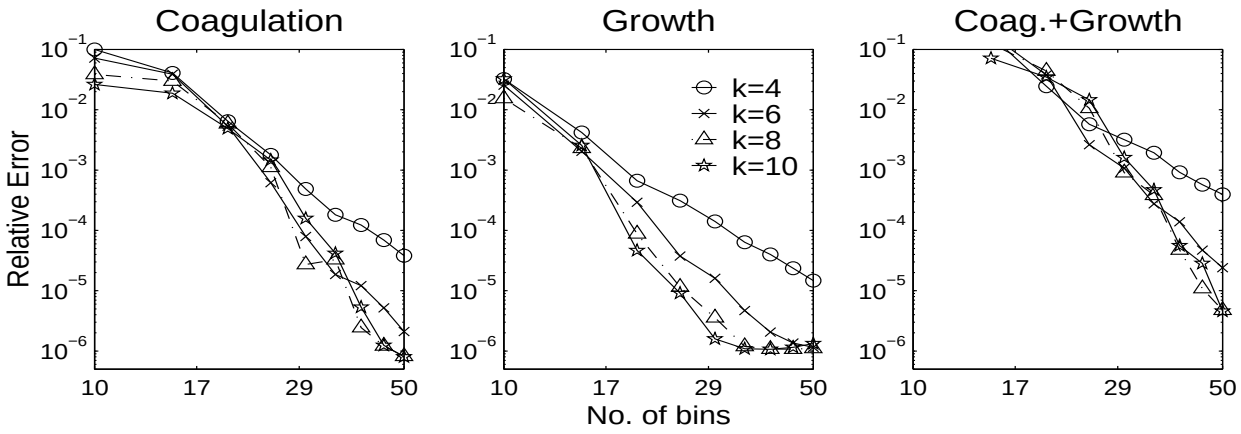

Figure 2: Experiment II (problem A in logarithmic coordinates). Accuracy of final solutions ($t_{\text{final}} = 6$ hours) versus the number of bins for coagulation only, growth only, and coagulation-growth problems. Splines bases of different orders are considered.

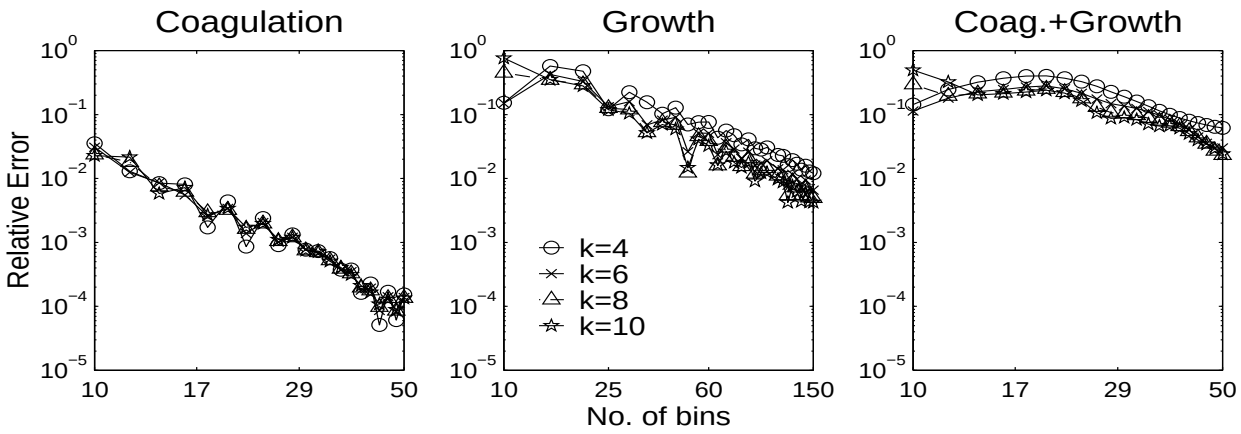

Figure 3: Experiment III (problem B). Accuracy of final solutions ($t_{\text{final}} = 1$ hour) versus the number of bins for coagulation only, growth only, and coagulation-growth problems. Splines of different orders show similar convergence rates.

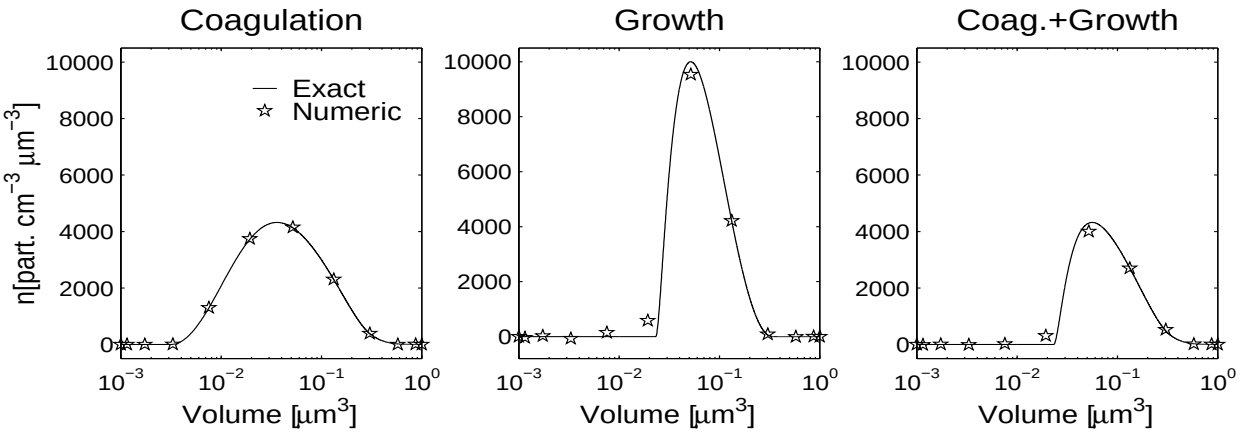

Figure 4: Experiment III (problem B). The reference and the numerical solutions at $t_{\text{final}} = 1$ hour for coagulation, growth, and coupled problems. The numerical solutions correspond to s=12 and k=6.

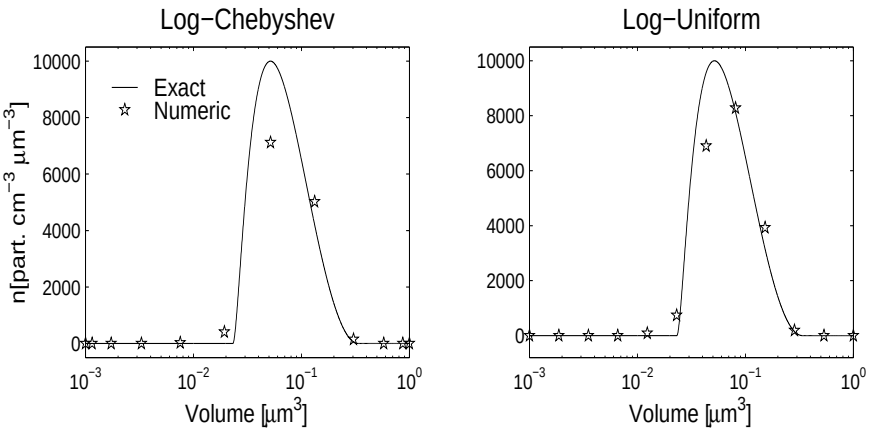

Figure 5: Experiment III (problem B). The reference and the numerical solutions at $t_{\text{final}} = 1$ hour for the growth problem solved with a flux-limited scheme. The numerical solutions shown correspond to s=12 and k=6. Log-Chebyshev and log-uniform collocation points are considered.

Spline Order (k)		4	6	8	10
Experiment I	coagulation	4.58	7.15	8.88	12.52
	growth	4.37	6.76	8.63	10.71
	coag.+growth	4.78	7.29	9.74	11.97
Experiment II	coagulation	5.16	7.21	7.75	9.96
	growth	4.59	5.76	7.89	9.26
	coag.+growth	4.68	7.39	9.30	9.35
Experiment III	coagulation	3.22	3.28	3.27	3.33
	growth	1.21	1.29	1.49	1.65
	coag.+growth	2.05	2.62	2.82	2.62

Table 1: Experimental orders of convergence for the three experiments.